UC San Diego

University of California, San Diego
PHYS 235, Spring 2022

To Self-Organized Criticality and Avalanching

Lecture by Professor P. H. Diamond

Summary by R. Masline

May 27, 2022 - June 6, 2022

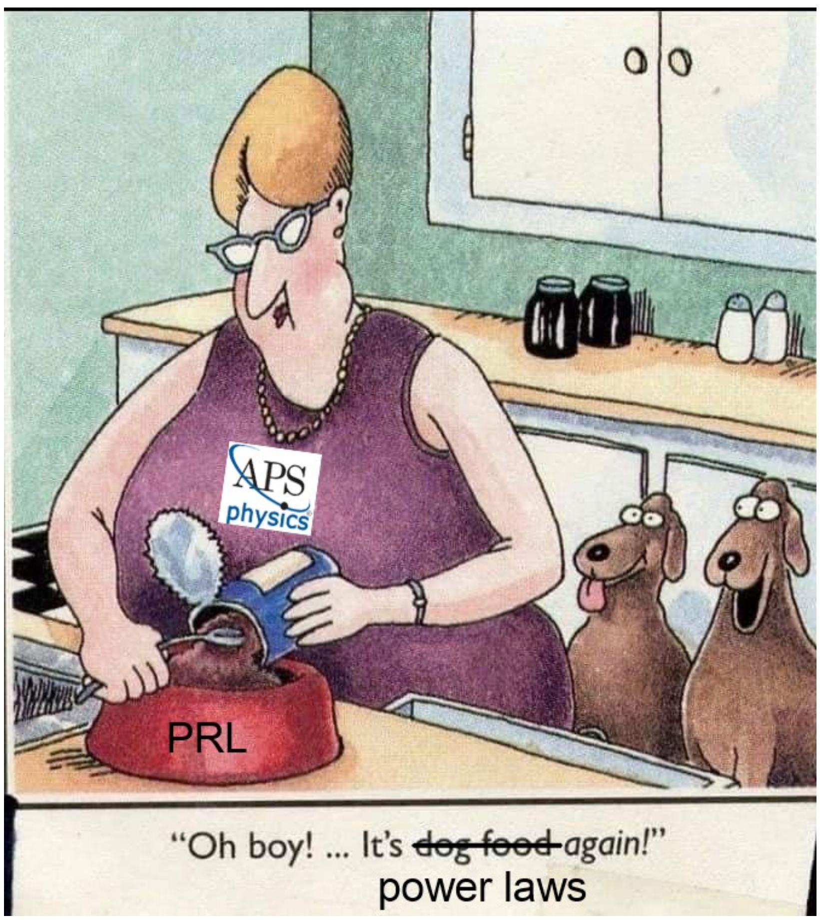

Hungry physicists wait to enjoy yet another feast [1].

Contents

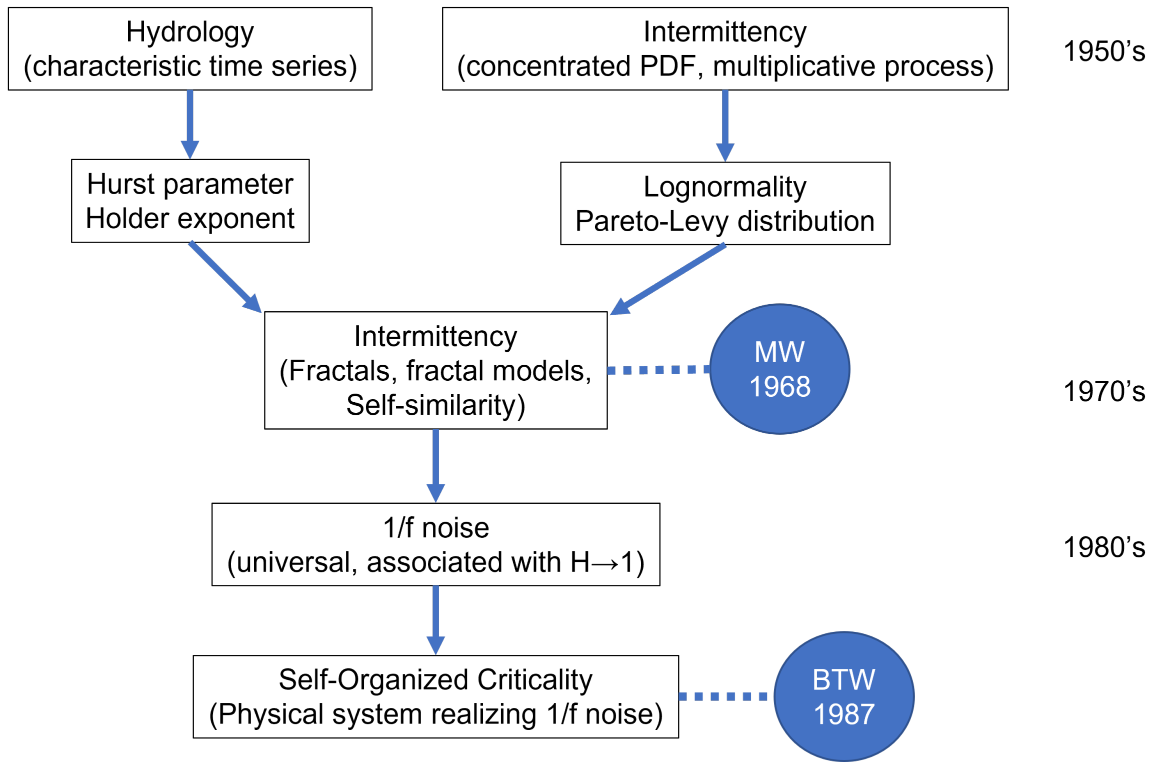

Figure 1: Story time with SOC.

1 What's going on?

1.1 Where we've gone: a brief intellectual history of SOC

It is useful to reassess our bearings and explicitly reaffirm what we've learned up until this point to provide a strong foundation as we move forward. As we continued our study of transport from diffusion to percolation and into the field of intermittency, we explored many different aspects of "usual" and "unusual" transport. Our journey is outlined in Figure 1, starting out as two distinct "storylines", merging in a single path towards self-organized criticality: a physical system realizing $1/f$ noise. Our first storyline has roots in hydrology, where Hurst and Holder described unusual behavior in time series, characterizing memory and non-diffusive behavior. The second storyline follows the long-standing problem of intermittency, looking at multiplicative processes and lognormality, featuring power-law and Pareto-Levy distributions. Pareto was looking at concentrated distributions (in particular, he looked at concentration of wealth in the economy) and Levy sought to generalize the central limit theorem, ultimately characterizing the Levy walk.

These two stories ultimately converged in fractal models, characterizing intermittency in self-similar systems by introducing a generalized dimension. This fractal model, which was championed by Mandelbrot, could unify both the time series dependence and turbulence with the intermittency, extracting a relationship between spatial and temporal self-similar structures and providing an effective model for the "weirdness" in temporal problems.

Chugging ahead, it was widely observed that many systems where $H \to 1$ exhibited a characteristic

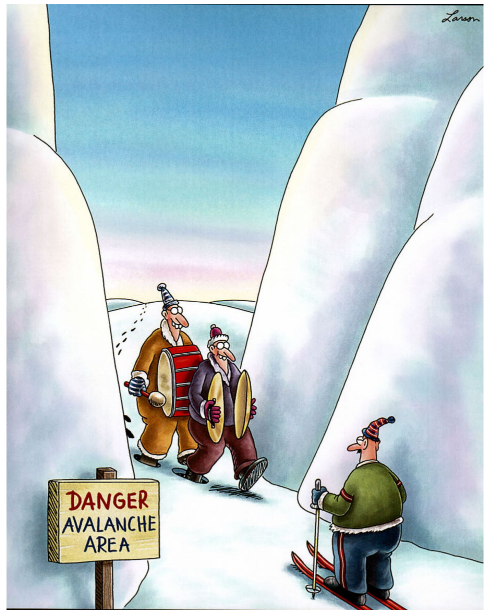

Figure 2: Experimentalists in 235 [1].

$1/f$ noise, which manifested a path forward to model anomalous scaling. Systems where $H \to 1$ describe ballistic propagation, where $\delta l \sim t$, suggesting self-similar characteristics. The search for a physical model that manifests this $1/f$ noise led to the development of the model of self-organized criticality (SOC), which is a state of self-similar **avalanching** (see Figure 2). SOC was first characterized and gained traction in the 1980's-1990's, with applications in the playground sandbox, physics (including our beloved confinement fusion), and other fields, as well as with politician Al Gore (stay tuned).

1.2 Where we're going: avalanching and building SOC

1.2.1 What is avalanching?

Before we get ahead of ourselves with discussions of both convenient and inconvenient truths, it is important to understand what an avalanche means for us. We define avalanche to be a relaxation event on some scale (let's call it l) bounded below by the correlation length of the system Δ_c, which is how big the basic cells are, and the system size L, or $\Delta_c < l < L$. Notice that the avalanche has a wide dynamic range: L/Δ_C, in the spirit of something like a Reynold's number. Appropriately, the distribution of avalanches is a power law.

1.2.2 Building blocks of SOC

The avalanche is like a sandpile, or a set of correlated overturnings, that lends itself to multiplicative models. Two key elements of the SOC model are Zipf's law and $1/f$ noise, which are related, but ultimately different.

We discussed Zipf's law previously in the course. Zipf's law states that the probability of an event is proportional to the reciprocal of the system size, that is, $P(x) \sim 1/x$. This tells us that that large events are rare, and small events are ubiquitous. Zipf's law fits a log-normal distribution for a broad finite range, which his natural for multiplicative processes [2].

This is similar to universal and ubiquitous $1/f$ noise, the driver behind avalanching. Looking at $1/f$ noise leads to a similar conclusion that large events are rare, and small events are frequent. Both Zipf and $1/f$ embody self-similarity and describe intermittent phenomena, and are related to the Hurst exponent. However, $1/f$, also called "shot" or "flicker" noise, describes the behavior of the frequency spectrum, where $\langle x^2 \rangle \sim 1/\omega$, while Zipf's law just characterizes the distribution.

Finding $1/f$ is not easy to get by the standard model. The "usual crank" approach is insufficient; a purely random process will have the auto-correlation function

$$\langle \phi(t_1)\phi(t_2)\rangle_n \sim |\phi_0|_k^2 e^{-i\omega_k(t_2-t_1)} e^{-|t_2-t_1|/\tau_c}. \tag{1}$$

Taking only the real frequency part (and ignoring the wave component), and Fourier transforming, we see that

$$S(\omega) = \frac{1/\tau_c}{\omega^2 + 1/\tau_c^2} \sim \frac{1}{\omega^2}, \tag{2}$$

as τ_c becomes large. This is a problem for $1/f$ noise, since τ_c introduces a timescale, while $1/f$ is scale-free. To remedy this, introduce a distribution of τ_c, reflective of an ensemble of random processes:

$$S(\omega) \sim \int_{\tau_c 2}^{\tau_c 1} P(\tau_c) S_{\tau_c}(\omega) \mathrm{d}\tau_c, \tag{3}$$

where $P(\tau_c)$ is the probability that τ_c occurs within our interval, $d\tau_c$, since τ_c is now probabilistically distributed rather than having a single characteristic correlation time. To force scale invariance, let $P(\tau_c) = \mathrm{d}\tau_c/\tau_c$, such that

$$S(\omega) = \int_{\tau_c 2}^{\tau_c 1} \frac{\mathrm{d}\tau_c}{\tau_c} \frac{1/\tau_c}{\omega^2 + 1/\tau_c^2} \mathrm{d}\tau_c = \left.\frac{\tan^{-1}(\omega\tau_c)}{\omega}\right|_{\tau_c 1}^{\tau_c 2} \sim \frac{1}{\omega}, \tag{4}$$

which recovers $1/f$. But what does this mean? We still don't have a physical scale or relation or idea. We want something that captures "Noah" and "Joseph" effects in non-Brownian random processes, as $H \to 1$, and displays $1/f$ noise.

2 Self-Organized Criticality

2.1 Bringing it all together

As it turns out, dynamical systems with many degrees of freedom will naturally evolve into a self-organized critical state, and the dynamics of such systems can be described with $1/f$ noise, which we will explore in the following sections. As a concept, SOC was floating around for a while before being "pinned down" in a 1987 paper by Bak, Tang, and Weisenfeld - or "BTW" - called "Self-Organized Criticality: An Explanation of $1/f$ noise" [3]. As the title would suggest, the BTW paper connected $1/f$ noise to SOC, where they suggest that the dynamics of the critical state is $1/f$ noise, and the dynamic criticality of the state can be characterized through many spatial degrees of freedom and fractal objects. Nominally, we use "$1/f$" to refer to $1/f^{\beta}$, where $\beta \leq 1$, reflective of the power-law spectrum.

2.1.1 Reaching the critical state

These processes involve a statistical ensemble of stimuli that lead to avalanches, which are spatially extended excitations that have wide-reaching effects across a whole systems. A system will evolve to a self-organized critical structure of states, which is marginally stable, meaning that the system will be stable relative to continuing fluctuations or overturning. A SOC system will exhibit power law scaling without tuning, and the system will evolve towards this state by itself, regardless of initial condition or distance to equilibrium.

Several key elements of SOC:

1. Motivated by $1/f$: universal and scale-invariant
2. Spatially-extended excitations (avalanches)
3. Collective ensemble of avalanches is intrinsic
4. SOC state: one of clusters that are dynamically marginally stable (as defined by the impulse response)
5. Power law for temporal fluctuations - reflects dynamical stability and scaling
6. Noise is necessary to probe the dynamic state: noise propagation through system via a "domino" effect on minimally stable clusters (reflects space-time propagation of avalanching events)
7. Critical point is attractor that is reached far from equilibrium (initial condition does not matter)
8. SOC state is marginally stable, but not *linearly marginally stable*, like the ITG or the β limit: the SOC state is dynamic
9. Critical structure is self-organized: unlike Ginzburg-Landau theory (where temperature is tuned as a parameter for a phase transition) the SOC structure (with $1/f$ noise and fractal objects) will tune itself

2.1.2 Percolation, but dynamic

Characteristics of the avalanche might sound familiar to percolation, discussed earlier in the course. The avalanche is the counterpart of a percolation cluster: it is like an ensemble of percolation clusters that span the system size. An avalanche will span the system's entire range of scales, from Δ to L, and "wants" to relax the gradient. It is not a perfect comparison, however, because unlike percolation, that avalanches are dynamic, and avalanches have some sense of direction. Directed

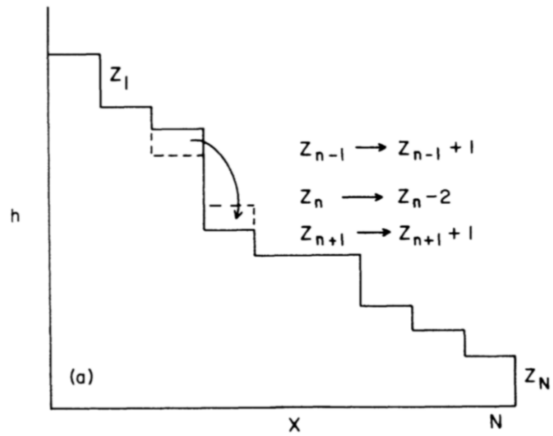

Figure 3: One-dimensional "sand-pile automaton. " The state of the system is specified by an array of integers representing the height difference between neighboring plateaus. There is a wall at the left and sand can exit only at the right. From [4].

percolation, which has a "direction" in time, is more similar to avalanching than "garden variety" percolation, but avalanching goes beyond directed percolation because it also relaxes the gradient.

2.2 Sandpiles

The idea of sandpiles is to use a familiar model to look for a minimally stable cluster. The sandpile is just a set of points reached by the toppling of a single site. Think of a grain being put on a pile of sand, and the pile of sand can collapse.

2.2.1 One dimension

We will start with the one-dimenstional lossy cellular automata model of a sandpile, proposed by Kadanoff [5]. This model features a box, with many cells in the box, and a random sprinking of sand or grains into the top of the box. The box is anisotropic, and the box is much larger than the individual cells in the box. One side of the box is a hard boundary (on the left) and the opposite side is open, which is the "lossy" boundary where grains are expelled if they go beyond the boundary. The sand pile is assembled by randomly adding grains to the pile, as in Figure 3. As shown in the figure, the vertical axis represents the height of the sand pile h, while the horizontal axis is broken up into N sites, where each site has a width of ΔX. We will define z_n as the height of each cell. The sand will be sprinkled into the box and will pile up to the one-sided heap shown in Figure 3. Eventually, the sand pile will reach a critical slope, where any new addition of sand will be sloughed off towards the lossy boundary side and ejected from the system. If $z_n - z_n + 1 > \Delta z_{crit}$, then the "automata rules" or "toppling rules" are:

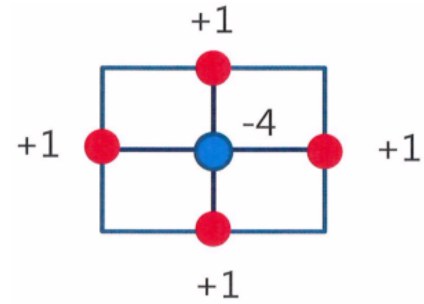

Figure 4: Once a site reaches the critical threshold, grains move from that site to the surrounding sites.

$$
\begin{aligned}
z_{n+1} &\to z_{n+1}+1 \\
z_n &\to z_n - 2 \\
z_{n-1} &\to z_{n+1} - 1.
\end{aligned} \tag{5}
$$

In this arrangement, any particles added after z_{crit} is reached will fall from state to state until they are ejected from the system when they reach the lossy boundary, meaning that this is the minimally stable state of the system. This is similar to an instability criterion, reminiscent of turbulent transport in magnetic confinement. We will return to this idea soon.

2.2.2 Two dimensions (and beyond, with enough computers)

A similar approach can describe sandpiles in two dimensions. The 2D cellular automata model (the model shown in BTW) showed a grid, with a rule in each lattice structure, such that if $Z > Z_{crit} = K$,

$$
\begin{aligned}
Z(x,y) &\to Z(x,y) - 1 \\
Z(x \pm 1, y) &\to Z(x \pm 1, y) + 1 \\
Z(x, y \pm 1) &\to Z(x, y \pm 1) - 1,
\end{aligned} \tag{6}
$$

where K is the critical threshold in occupation (**not** a gradient threshold). In other words, if the occupation went above a certain critical value, you chop off four grains from a point and shift them to all sites around it, like in Figure 4.

If the threshold is exceeded, particles will get shifted to the adjacent neighbors in each direction. This means that one grain can have far-reaching effects in both dimensions, since the perturbation will propagate to the neighbors of the "toppled" cells, and in turn, could topple to their neighbors, and so forth. This is unlike the sandpile problem, which was minimally stable with respect to small fluctuations, where the perturbation will cause an ejection of particles to the lossy boundary. Instead, the the 2D system has a cascade-like effect in response to a fluctuation, meaning that the 2D system will settle into a SOC state with minimally stable clusters, where a cluster is set of points reached by toppling *one* cell. Stability is reached when these minimally stable clusters have been

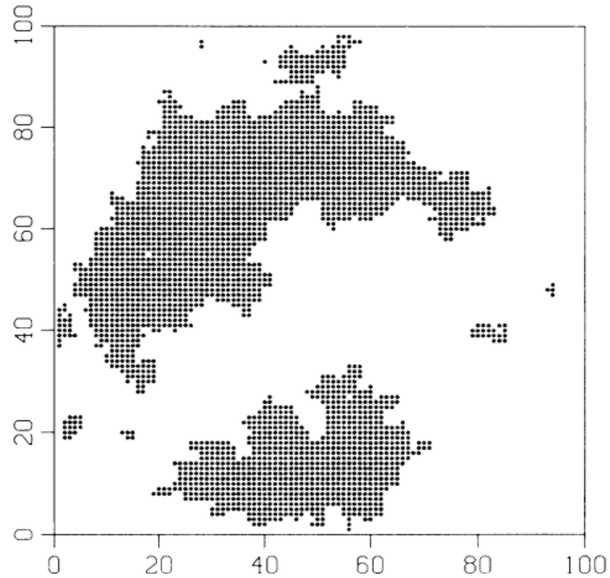

Figure 5: Self-organized critical state of minimally stable clusters, for a 100x100 array. From [3].

broken down to the point where the fluctuation or noise cannot propagate across infinite distances [3]. Since there was never any specific length scale introduced in this problem, the structure of the minimally stable states is scale invariant.

The distribution of these cluster sizes scales with a Zipf distribution, and there are a few big ones and many small ones. Shown in Figure 5, each dark structure encompasses any point response to a single input and response to that one input. Fractals are evident in final state [3].

This system shows us that there is a combination of dynamical minimal stability and spatial scaling, which leads to a power law distribution for the temporal fluctuations. These temporal fluctuations propagate through the scaling clusters with a "domino" effect (the cascade), which is the avalanche. In 2D, the avalanche propagates and dynamics change in both space and time, eventually reaching the "attractor" state despite starting far from equilibrium.

2.2.3 Metaphysical dimensions

The author would like to note that like any other physicist, she loves to hear herself talk (or in this case, write). However, she acknowledges that she cannot be "out-talked" by a politician, and will leave the characterization of metaphysical sandpiles to its author in his own direct words. Former Vice President Al Gore says in his book *Earth in the Balance*:

> "The sandpile theory-self-organized criticality-is irresistible as a metaphor; one can begin by applying it to the developmental stages of human life. The formation of identity is akin to the formation of the sand pile, with each person being unique and thus affected by events differently. A personality reaches the critical state once the basic contours of its distinctive shape are revealed; then the impact of each new experience reverberates throughout the whole person, both directly, at the time it occurs, and indi-

Kadanoff Model	**MFE**
Pile	Confinement
Grid site/cell	Local fluctuation/eddy
Toppling/automata rules	Local instability/turbulence mechanism
$\Delta_{L,crit}$	"Critical Gradient" for instability ($\nabla L_{crit} \to$ transport; $1/L_{crit}$
N (number of grains toppling)	Eddy mixing rule
Random rain of grains	External heating (random input to the system as heating $\to$ SOC)
Sand grain flux	Heat/particle flux
Average slope	Mean profile
Avalanche	Avalanche
Sheared wind	Sheared electric field
Fractal profiles	Choppy profiles
Local rigidity	Profile stiffness

Table 1: Similarities between the Kadanoff model and turbulence.

> rectly, by setting the stage for future change .... One reason I am drawn to this theory is that it has helped me understand change in my own life."

To which Per Bak, the "**B**" in "BTW" [6] remarks,

> "Maybe Gore is stretching the point too far."

Take that as you will.

2.2.4 Analog to Turbulence in MFE

Another phenomenon that exhibits similar (although not identical) avalanching behavior to the Kadanoff 1D sandpile model is turbulence. The dynamics of the Kadanoff model become "interesting" when $\Delta x/L << 1$, or the cell size is much smaller than the scale length of the system. This is analogous to turbulence, where $\rho^* << 1$. In turbulence, transport is also spatially extended, and things move if you exceed the instability criterion. Other similarities are summarized in Table 1.

However, this comparison isn't perfect. Purists would say that the criticality condition for turbulence is $1/L_t > 1/L_{t,crit}$, which is a scale length and not a gradient condition. Though critical gradient models exist, it is difficult to relate them to actual stability criterion (which are easier to formulate and understand). Another pitfall of this comparison is that when you exceed the critical threshold in the 1D sandpile, you topple, whereas in a system that could face turbulence, you have inertia. Ultimately, it's a useful phenomenology, but falls short of a true "one-to-one" comparison.

2.3 Honing in on SOC

Now that we have elaborated on the fundamental models used in analyzing SOC, what do they tell us? In identifying these mathematical toys, we can develop and hone in on a more precise definition of SOC. There are two approaches to defining SOC:

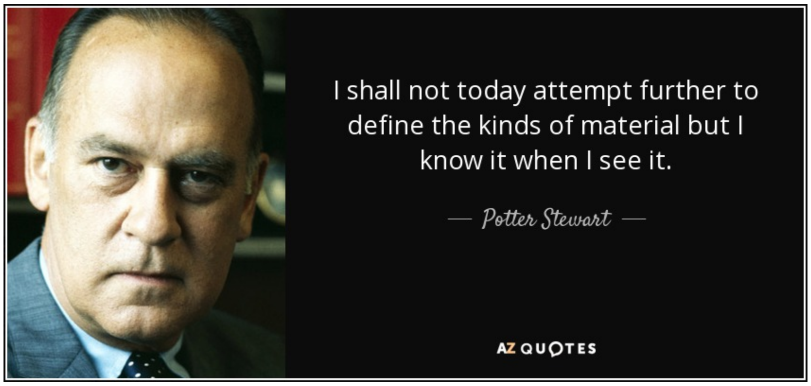

Figure 6: The United States Supreme Court on self-organized criticality, or something.

1. The **constructive definition** is that SOC is a slowly-driven, interaction-dominated threshold system. A classic example of this would be a sandpile, where one single grain can be perturbed or added to the pile and cause a global, system-wide toppling.

2. The **phenomenological definition** is more along the lines of Figure 6; it is a system exhibiting power law scaling without tuning.

The framework of these two definitions introduces several more key elements to SOC that can help us identify and understand critical systems:

1. These models show us that SOC is a slowly-driven, interaction-dominated threshold system (like a sandpile, where the addition or perturbation of a single grain can topple the whole pile).

2. SOC states are interaction-dominated, leading to global transient excitation; they have many degrees of freedom, since they have many cells or modes, so their dynamics are dominated by couplings between the cells and degree of freedom interactions.

3. There is a need for both a threshold and slow drive.

   (a) The threshold is a local criterion for excitation, in that the excitation happens not through the system directly, but through one cell. It is a threshold in occupation, and not a gradient threshold, meaning that if you exceed that threshold, particles will get shifted to various neighbors.

   (b) Slow drive is necessary to actually see the dynamic effects of the perturbation on the system, rather than obscuring the response by dumping over it too quickly. A strong drive would bury the threshold, while the slow drive uncovers the threshold marginality. The "strength" of the drive is set by the toppling rules, fueling, and box size.

4. There are a large number of accessible, meta-stable, quasi-static configurations.

5. The local profiles are rigid, much like profile stiffness in magnetic confinement, where the actual profile in a marginal state will be proximal to the location of the local SOC state (although the precise relation of the SOC state to the marginal state is unknown).

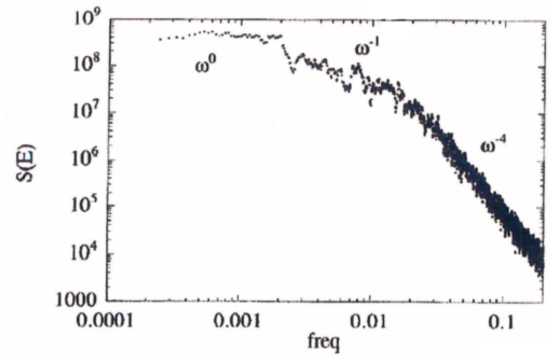

Figure 7: Power spectrum of over-turnings, $\langle(\Delta Z)^2\rangle_\omega$.

6. Once again, there is a power law that is inextricably linked to the self-similarity, and SOC is related to Zipf's law and $1/f$ noise.

2.4 Generic results of SOC

2.4.1 Power spectrum

Speaking of $1/f$ noise, SOC exhibits a generic structure in power spectra, with large power in the slowest, lowest frequencies, shown in Figure 7. The $1/f$ range manifests in the middle of the spectrum, reflective of the self-similar, interaction dominated "Joseph" events. The lowest range, ω^0, characterizes the intermittent "Noah" events, where most of the power is generated. The ω^{-4} range is self-correlation dominated, since it corresponds to localized, uncorrelated overturning events.

2.4.2 SOC vs. Marginal

The SOC state is not the marginal state, but the SOC state is close to the marginal state at the boundary. As "stuff" rains into the profile, it will eventually begin to topple and goes out, because of the lossy boundary, as in Figure 8. Any avalanche in this system either dies out, or hits that edge. Because of this, the fate of all the transport in the system *has* to hit the lossy boundary region, which is very interaction-dominated. The probability isn't necessarily any higher at the boundary, but whatever gets sprinkled in at any region will inevitably go through the lossy boundary as the system shifts and changes, meaning that it will be strongly interaction-driven at that boundary and not necessarily wholly governed by the raining conditions set out by the problem. This area will be more like the marginal state, since it isn't governed by the usual dynamics of the whole SOC profile. Because of this, toppling events will be more frequent at the boundary.

3 Hydrodynamic models

SOC is intimately connected with self-similarity, which is an important element of the cascade. Cascades are rooted in turbulence and connected to fluid mechanics. The SOC events we have discussed up until now have been based on ideas like the sandpile, but it would be useful to construct

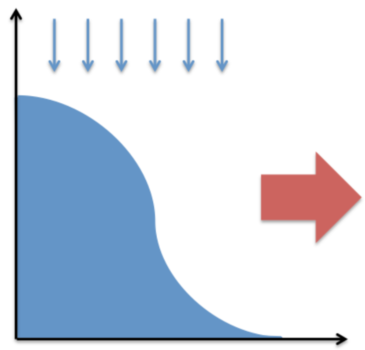

Figure 8: All particles will travel through the lossy boundary and will be ejected from the system.

a continuum model, which would be relevant when $L_{\text{avalanche}} >> \Delta_{\text{cell}}$. Building on our sandpile model, this would be like granular flow, or the flow of sand, and would be applicable if there is interest in large scale dynamics relative to a grain of sand.

Ideally, we would like to search for a formulation akin to the Ginzburg-Landau theory that relies on symmetry, but without tuning. The set of symmetry considerations in the Ginzburg-Landau theory dictate the form of the free energy, which is why it can be applied universally (as opposed to twiddle-terms often used in fusion, that vary from system to system). Ginzburg-Landau says

$$\frac{\mathrm{d}\eta}{\mathrm{d}t} - D\nabla^2\eta = -(T - T_c)\eta - b\eta^3, \tag{7}$$

and we can use this framework to develop a continuum, hydrodynamic model of SOC, reminiscent of Burgulence (Burgers turbulence). We need this model to apply for a self-tuning system (i.e. no tuning for the temperature to induce the state change, like in the Ginzburg-Landau equation), and we need the model to work on scales $L > l > \Delta$ and $\tau_{confinement} > \tau > \tau_{step}$.

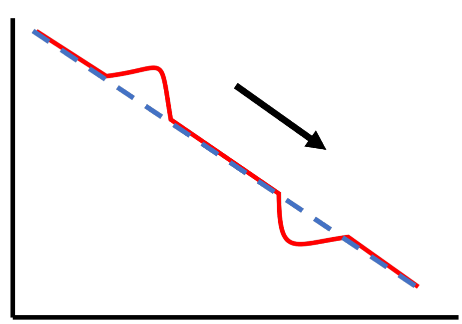

Figure 9: The SOC profile. The blue line represents the SOC profile, while the red line represents the deviations introduced by the noise.

Figure 10: Various holy books.

3.1 Flipping burgers

To formulate this model, we will look at a one-dimensional box with an ejecting boundary on the right-hand side and an accumulating boundary on the left. This model has a SOC profile, but we don't know what it is, and the model can't predict it. The model can, however, predict the fluctuations, so we can sprinkle noise as some random rain into the system, unlike BTW, which had a single perturbation. We will see deviations from the marginal profile, which will manifest as excesses, blobs[1], bumps, or clumps (for positive deviations) and deficits, voids, holes, or depletions, as in Figure 9.

This creates a dynamic profile of excesses and deficits, where variations can be up or down. There are no a priori self-binding mechanisms, just fluctuations that can either go up or down the profile. Profile fluctuations manifesting as excesses or deficits at the edge had been observed at the edge of fusion experiments before [7], but the dynamics of the variations were recently confirmed by Minjun J. Choi, who showed that voids will move up the profile and bumps will move down [8].

3.1.1 Order parameter

To continue building our model, we can introduce an order parameter:

$$\delta P = P - P_{soc}, \tag{8}$$

which represents the local excess or deficit. We want to track how this deficit evolves, so grab your spatula and prepare to start flipping burgers. We will start with the governing equation for P, the system occupation, or the density of stuff:

$$\partial_t \delta P + \partial_x \Gamma(\delta P) - D_0 \partial_x^2 \delta P = \tilde{S}, \tag{9}$$

where $\Gamma(\delta P)$ is the flux associated with the deviation from the SOC profile - above SOC critical state, we get a bump, and below, we get a void. This gives us a simple hydrodynamic equation that

[1] Use this term at your own risk. See Figure 10 and assess the consequences here. You have been warned.

will characterize SOC for us (we can also translate this into higher dimensional models; see [9] - useful in confinement when the most interesting direction is radial, across the flux surface). The δP is conserved to the $\tilde{S}$ boundary, but we can constrain δP by symmetry.

3.1.2 Joint reflection symmetry

We notice from Figure 9 that $\delta P > 0$ gives us a bump or excess that tends to move down the gradient to the right towards and through the ejecting side, since there is a greater extent on the down-slope (the right-side "base" of the bump) due to the asymmetry introduced by the lossy boundary. Conversely, $\delta P < 0$ gives us a void or deficit that tends to move up the gradient to the left, since the steeper slope is on the left-hand side. In general terms: bump goes out, void goes in.

If we induce a spatial interchange ($x = -x$), we would get a reflection of the system. If we *also* interchange our order parameter ($\delta P = -\delta P$) with our spatial interchange, we see that the direction of $\Gamma(\delta P)$ would be unchanged: flipping the pile and the blobs would give us the same behavior as the original system. This is symmetry, which allows for significant simplification of the flux, since $\Gamma(\delta P)$ is invariant under $x = -x$ **and** $\delta P = -\delta P$.

The general form of the flux is:

$$\Gamma(\delta P) = \sum_{m,n,a,r,\alpha} \{\underbrace{A_n(\delta P)^n}_{1} + \underbrace{B_m(\partial_x \delta P)^m}_{2} + \underbrace{D_\alpha(\partial_x^2 \delta P)^\alpha}_{3} + \underbrace{C_{q,r}(\partial_x P)^q(\partial_x \delta P)^r}_{4} + \ldots\} \tag{10}$$

We want to find the flux in the large-scale, long-time limit, so we are looking for the smoothest form of the flux, or the flux with lowest order of derivatives. The higher order derivatives are more and more sensitive to the fine structure of the pile profile, which isn't necessary for our focus on large spatial and time scales. We want only the simplest form. Since we have shown that we have joint reflection symmetry, we can start to cull the herd of terms with symmetry. For each part of the equation:

1. The $n = 1$ term violates JRS. If we flip the sign of δP, the flux changes sign. Kill. The $n = 2$ term is okay.
2. Derivatives of δP are okay if $m = 1$ and $m = 2$, since the product of x and δP is invariant under reflection.
3. If $\alpha = 1$, this term violates the joint reflection symmetry. Kill. The $\alpha = 2$ term is okay, so we keep it. For any larger α, the scale is too small to be considered. Kill.
4. The only relevant terms are $q = 1$ and $r = 1$, otherwise there is an unnecessary emphasis on fine scales. Single powers of terms would violate joint reflection symmetry. Kill.

Taking the survivors, Eq. (9) is now

$$\partial_t \delta P + \partial_x[A_2(\delta P)^2 + B_1(\partial_x \delta P) + B_2(\partial_x \delta P)^2 + D_2(\partial_x^2 \delta P)^2] - D_0 \partial_x^2 \delta P = \tilde{S}. \tag{11}$$

We can combine several of the constants (since they are of the same form) and eliminate some of the lower-order terms that describe the smaller scales. Finally, we arrive at our goal:

Figure 11: Tidal bores. From [10].

$$\partial_t \delta P + \partial_x[\alpha \delta P^2 - D\partial_x \delta P] = \tilde{S}, \tag{12}$$

a noisy Burgers equation that supports shocks and shock trains. Shocks produce entropy and correspond to relaxation, which is akin to our understanding of avalanches. While not *exactly* the same, a shock can be visualized like bores in water flow, shown in Figure 11. The "ripple" series of the bores is like a shock train. In a shock, mass, momentum, and energy are conserved, while bores only conserve mass and momentum, and the energy goes into turbulence at the front of the bore. This is similar to what happens in an avalanche, which will "burgle" along but look like a hydraulic jump.

3.2 Avalanche turbulence

It should be no surprise that SOC has infrared characteristics; we are dealing with a system with $1/f$ behavior. We have a noisy Burgers equation to describe the deviation from the SOC state, which tells us that we can basically achieve relaxation by shocks (or in our case, avalanches), and turbulence is an ensemble of these shocks. An avalanche is essentially a shock train that steepens.

3.2.1 Renormalized viscosity

With the presence of noise, we can calculate an effective dissipation rate as a function of scale. It would be useful to obtain an effective diffusivity that describes the δP^2 term, which characterizes the nonlinearity, N. We can start to analyze Eq. (12) to look for a long wavelength approximation to nonlinear flux, or

$$[\partial_x(\alpha \delta P^2)]_n \to \mathrm{d_n} \delta P_n \simeq \nu k^2 \delta P_n, \tag{13}$$

where ν is a turbulent viscosity. We can calculate ν through quasilinear theory. Assume one of the δP's is large relative to the other, and we can "quasilinear-ize" to get a viscosity-looking term, and then Fokker Plank the result to get a resonant diffusivity.

Applying this procedure gives a turbulent viscosity

$$\nu_T \simeq \sum_{k',\omega'} |\delta P_{k',\omega'}|^2 \frac{k'^2 \nu_T}{[\omega^2 + (k'^2 \nu_T)^2]}. \tag{14}$$

This viscosity is defined recursively, meaning the viscosity is non-Markovian and there is some memory in the system.

Now, we can related δP to the noise (where the high-frequency, short wavelength modes excited). It must also include the non-linear response, self-consistently. Let $(-i\omega + k'^2\nu)\delta P_{k',\omega'}) = \tilde{S}_{k',\omega'}$, such that Eq. (14) becomes

$$\nu \simeq \alpha^2 \sum_{k',\omega'} \frac{|\tilde{S}_{k',\omega'}|^2}{(k'^2\nu)^3} \frac{1}{[(1+(\omega'/\nu k'^2)^2]^2}. \tag{15}$$

If we take

$$\sum_{k',\omega'} = \int_{k_{min}}^{\infty} dk' \int d\omega' \tag{16}$$

and

$$|\tilde{S}_{k',\omega'}|^2 = S_0^2, \tag{17}$$

we get white noise. Our viscosity now changes to

$$\nu = \frac{c_1 \alpha^2 s_0^2}{\nu^2} \int_{k_{min}}^{\infty} \frac{dk'}{k^4}, \tag{18}$$

which manifests infrared divergence, resulting from the conserved order parameter and slow modes. The weak noise and tiny density give strong intensity. The general point is that weakly damped modes are still dangerous, if any excitation is available.

4 SOC in MFE

4.1 Simulations

Here, we have made the case for SOC, but there is a global anisotropy in interest in SOC phenomena. SOC and avalanching attract much more attention in Asia and parts of Europe than anywhere else. Ultimately this is most likely because of the codes used in various laboratories and research groups. To get an avalanche *right*, you need to correctly evolve the gradient, without approximating assumptions. Since the profile is dynamic in avalanches, you need gyro-F codes that can correctly model evolving gradients.

Since measuring avalanches in experiments is difficult, simulations provide insight into the physics of the avalanche, but they have to correctly model the evolution of the fluxes. The first simulations to get the avalanche right were resistive fluid models that were simulating resistive interchange turbulence in a cylinder using a code similar to BOUT++, which is a multifluid modelling code that is flux-driven [11].

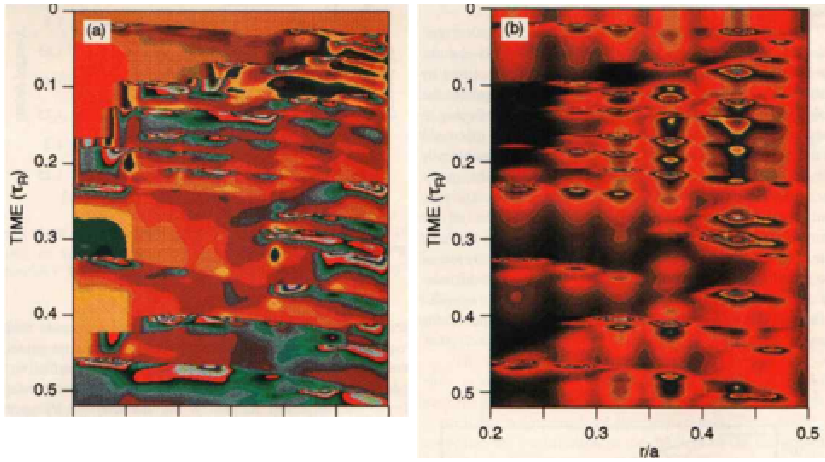

Figure 12: The vertical axis is time and the horizontal axis is radial position. In this plane, we plot (a) averaged pressure contours and (b) rms potential fluctuation contours. From [11].

The results of these simulations (shown in Figure 12) show that avalanches are happening. In the rms potential contour, there are persistent vortices at low order rational surfaces, while in the pressure contour, order is more horizontal, with streak-like behavior. These are avalanches, or perturbations that have been extended in radius. The frequency spectrum, shown in Figure 13 looks very similar to that of the box power spectrum we looked at earlier in Figure 7, and the flux spectrum shows similar behavior.

Numerous other full-F flux-driven gyrokinetic simulations have produced similar results, and show that large portions of the fluxes are carried by avalanche events.

4.2 Experiments

Computer simulations are always fun, but what about physical experiments? Unfortunately, it isn't easy to get global profile dynamics since they are difficult to measure, and the direct imaging of avalanches is beyond present-day capabilities. Instead, experimental observations of avalanches must come from indirect measurements. Fluctuation profiles in I_{sat}, which are reflective of density fluctuations, show similar trends to Figure 7, indicating universality, but it's difficult to draw definitive conclusions without direct measurements.

The H-exponent can be measured for large tokamaks, since scale separations are large enough, but $H \sim 0.7$ is a general trend for large machines. This is detailed in Figure 14.

4.3 Avalanching vs. zonal flows

How do avalanches, which are radially extended collective events like a domino toppling, coexist with zonal flows? Zonal fows are noncontroversial (they are widely-observed and largely well-understood) poloidal bands of shear flows. There is a love-hate relationship between zonal flows and avalanching, in that zonal flows restrict avalanches, but avalanches can drive zonal flows, since transport drives zonal flows.

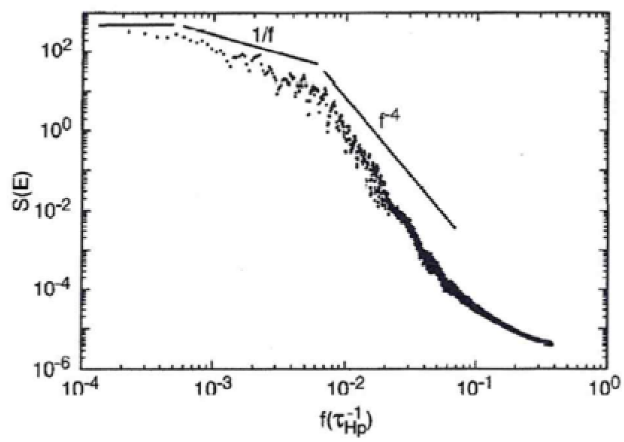

Figure 13: The electrostatic potential fluctuation spectrum at $r/a = 50.35$, $\theta = \pi/4$, and $\zeta = 50$. This spectrum has the three characteristic regions observed in the sand pile model. From [11].

Device	Number of time series	$\langle H \rangle_{\text{in}}$	$\langle H \rangle_{\text{out}}$	τ_D (μs)	Self-similarity range (ms)
TJ-1	9	0.75 ± 0.03	0.75 ± 0.04	3.0	0.1–2.0
JET limiter	4	···	0.52 ± 0.04	29.0	0.1–2.0
JET divertor	4	···	0.63 ± 0.03	19.0	0.1–2.0
TJ-IU stellarator	21	0.64 ± 0.03	0.67 ± 0.01	6.0	0.1–2.0
W7-AS $\iota_a = 0.243$	24	0.62 ± 0.01	0.60 ± 0.04	20.0	1–20
W7-AS $\iota_a = 0.355$	29	0.72 ± 0.07	0.66 ± 0.06	19.0	1–20
ATF	20	0.71 ± 0.03	0.92 ± 0.07	34.0	1–12

Figure 14: Measurements of H in various tokamaks. From [12].

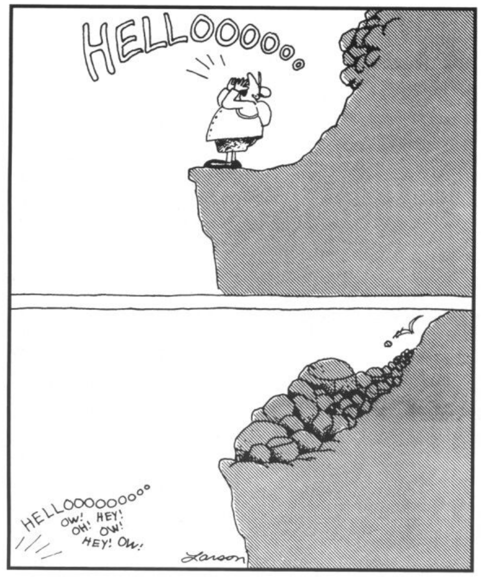

Figure 15: Staircase-like phenomena in transport is ubiquitous [1].

The empirical hint that transport drives zonal flows is the L-H transition, which is related to the onset of a strong shear layer at the edge of the plasma, met with the power threshold. Transport increases with power, since the scale of the transport is linked to the gyroradius, so transport will increase as the power threshold is reached. That critical power is necessary for the shear layer, but what is actually going on is a global pattern formation or selection problem. In other words, there are two possible secondary patterns: a zonal flow, from the increased transport, or an avalanche, from the criticality paradigm. It turns out, they *can* coexist, which is the $\mathbf{E}\times\mathbf{B}$ staircase.

4.3.1 $\mathbf{E}\times\mathbf{B}$ staircase

The $\mathbf{E}\times\mathbf{B}$ staircase is an analogue of the potential vorticity staircase, an outgrowth of meteorology and fluids, or the staircase shown in Figure 15. It's in the name, but the $\mathbf{E}\times\mathbf{B}$ staircase profile looks like a staircase, with flat spots of high transport and steep, nearly vertical layers acting as mini-barriers that coexist. These structures might not be so regular as the name "staircase" would imply, but it's helpful to visualise them like this to help us first understand. In our context, this means the avalanches happen in between the flat parts and the shear layers occur in the mini barriers. This isn't a decoupling of these phenomena, but rather a spatial phase separation (much like the Cahn-Hilliard equation, which describes the density contrast in two phases).

In a zonal flow, radial wave propagation generates momentum convergence (analogous to Reynolds stress) which will break up into zonal banding and cause the formation of stratified bands. The interaction of these structures with the turbulence can be formulated as a predator-prey system, where the zonal flows are the predator and the prey is the turbulence intensity. The zonal flow is symmetric and can't grow on its own, so it won't extract energy from the system directly. Instead the zonal flow is driven by non-linear couplings from the waves. This forms the basis for the predator-prey feedback loop, meaning that the zonal flow has self-feedback.

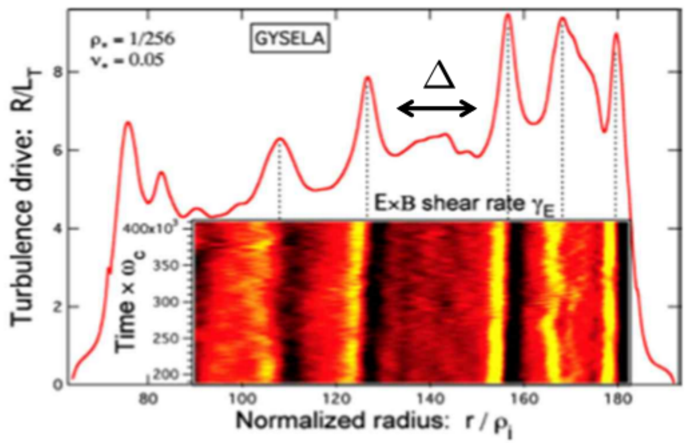

Figure 16: The $\mathbf{E}\times\mathbf{B}$ shear rate and turbulence drive reveal the staircase structure of the simulation profile.

But what about avalanching? Avalanching is diametrically opposed to the zonal flow, but both are claimed to exist. Having zonal flows are good, since there is no radial transport and they can act as a dump for energy that would otherwise interact with scales that can drive transport, but having avalanching is...questionable; avalanching can increase transport over local values and break Gyrobohm scaling. In reality, transport is somewhere between Bohm and Gyrobohm scaling, and avalanching would be perfect for explaining this. However, there is no quantatative link between avalanche dynamics and the Gyrobohm scaling exponent.

We have two secondary structures at work, both of which are driven by heat flux and the relaxation of the gradient. This is where the staircase formulation is useful: instead of a single layer, there is a lattice of layers and avalanches, complete with more beautiful sets of colorful, gorgeous simulation pictures. To see this, simulations require a full-f, flux-driven code, which reveals quasi-regular patterns of shear layers and profile corrugations, shown in Figure 16. In this figure, yellow and black represent the flow, where there is a rapid transition of the direction of flows around peaks in turbulence drive. This is the shear layer, which is interspersed with a regular pattern of shear layers and profile corrugations. These regions have local steepening, but in between, the flat spots correspond to areas where confinement is low. The flat regions are regions of avalanching, which are truncated by the onset of a new shear layer. This solves the coexistence problem by allowing both processes to live in segregated coexistence, like a phase separation of spinodal decomposition.

References

(1) Larson, G., *The Far Side*.
(2) Montroll, E. W.; Shlesinger, M. F. On 1/<i>f</i> noise and other distributions with long tails. *Proceedings of the National Academy of Sciences* **1982**, *79*, 3380–3383.
(3) Bak, P.; Tang, C.; Wiesenfeld, K. Self-organized criticality: An explanation of the 1/f noise. *Phys. Rev. Lett.* **1987**, *59*, 381–384.
(4) Bak, P.; Tang, C.; Wiesenfeld, K. Self-organized criticality. *Phys. Rev. A* **1988**, *38*, 364–374.
(5) Kadanoff, L. P. et al. Scaling and universality in avalanches. *Phys. Rev. A* **1989**, *39*, 6524–6537.
(6) Bak, P. P., *How nature works : the science of self-organized criticality*; Copernicus: New York, NY, USA, 1996 - 1996.
(7) Krasheninnikov, S. I.; Smolyakov, A.; Kukushkin, A., *On the Edge of Magnetic Fusion Devices*, 1st ed.; Springer: Cham, Switzerland, 2020.
(8) Choi, M. J. et al. Experimental observation of the non-diffusive avalanche-like electron heat transport events and their dynamical interaction with the shear flow structure. *Nuclear Fusion* **2019**, *59*, 086027.
(9) Hwa, T.; Kardar, M. Avalanches, hydrodynamics, and discharge events in models of sandpiles. *Phys. Rev. A* **1992**, *45*, 7002–7023.
(10) Tidal bore dynamics.
(11) Carreras, B. A. et al. A model realization of self-organized criticality for plasma confinement. *Physics of Plasmas* **1996**, *3*, 2903–2911.
(12) Carreras, B. A. et al. Long-Range Time Correlations in Plasma Edge Turbulence. *Phys. Rev. Lett.* **1998**, *80*, 4438–4441.